

# Studies of New Vector Resonances at the CLIC Multi-TeV $e^+e^-$ Collider

---

**Marco Battaglia**

*CERN, CH-1211 Genève 23, Switzerland*  
*E-mail: marco.battaglia@cern.ch*

**Stefania De Curtis**

*I.N.F.N., Sezione di Firenze, I-50019 Sesto F., Italy*  
*E-mail: decurtis@fi.infn.it*

**Daniele Dominici**

*Dipartimento di Fisica, Università di Firenze, I-50019 Sesto F., Italy*  
*I.N.F.N., Sezione di Firenze, I-50019 Sesto F., Italy*  
*E-mail: dominici@fi.infn.it*

**ABSTRACT:** Several models predict the existence of new vector resonances in the multi-TeV region, which can be produced in high energy  $e^+e^-$  collisions in the s-channel. In this paper, we review the existing limits on the masses of these resonances from LEP/SLC and TEVATRON data and from atomic parity violation, in some specific models. We study the potential of a multi-TeV  $e^+e^-$  collider, such as CLIC, for the determination of their properties and nature.

**KEYWORDS:** Beyond Standard Model, e+e- Experiments.

---

## Contents

<b>1. Introduction</b>	<b>1</b>
<b>2. <math>Z'</math> Boson studies</b>	<b>2</b>
<b>3. Study of the D-BESS model</b>	<b>6</b>
<b>4. Kaluza-Klein excitations in theories with Extra-Dimensions</b>	<b>9</b>
<b>5. Electroweak observables and sensitivity to <math>Z'</math> Boson and KK excitations</b>	<b>10</b>
<b>6. Conclusions</b>	<b>15</b>

---

## 1. Introduction

While the core of the physics program of a TeV-class linear collider (LC) can be already largely defined on the basis of what we know today, the signals from new physics which could be probed by a multi-TeV collider, such as CLIC [1] at  $1 \text{ TeV} < \sqrt{s} < 5 \text{ TeV}$ , belong to a significantly broader domain. Still, one of the most striking manifestation of new physics will come from the sudden increase of the  $e^+e^- \rightarrow f\bar{f}$  cross section indicating the s-channel production of a new particle. There are several theories which predict the existence of such a resonance. In this paper we study the sensitivity of CLIC to scenarios including new vector boson resonances. A first class consists of models with extra gauge bosons such as a new neutral  $Z'$  gauge boson. This is common to both GUT-inspired  $E_6$  models and to Left-Right (LR) symmetric models. They are discussed in Section 2. Models of dynamical electroweak symmetry breaking also predict the existence of new resonances in the TeV region. In particular, we consider the degenerate BESS (D-BESS) model, which describes a pair of narrow and nearly degenerate vector and axial-vector states [2], in Section 3. Additional resonances are also introduced by recent theories of gravity with extra dimensions in the form of Kaluza-Klein graviton and gauge boson excitations. A five dimensional extension of the Standard Model (SM) is discussed in Section 4. Beyond discovery, it will be essential to accurately measure their masses, widths, production and decay properties to determine their nature and identify which kind of new physics they manifest. The recently proposed little Higgs models, a new approach to the hierarchy problem, predict also new vector bosons in the TeV range, see for instance [3]. Their possible signature at a multi-TeV collider deserves further study. CLIC will also be sensitive to new vector gauge bosons at mass scales much beyond the kinematic threshold. In Section 5 we discuss the statistical accuracy for the determination of the cross sections,  $\sigma_{f\bar{f}}$ , and forward-backward asymmetries,  $A_{FB}^{f\bar{f}}$ , for  $\mu^+\mu^-$ ,  $b\bar{b}$  and  $t\bar{t}$  at  $\sqrt{s} = 3 \text{ TeV}$ . These accuracies will be used to establish the sensitivity reach to indirect effects of new vectors as  $Z'$  gauge bosons and Kaluza-Klein excitations of the photon and of the  $Z^0$  boson.

Extra-U(1)	LR ( $g_L = g_R$ )
$v'_e = -\frac{1}{4}s_\theta \left( c_2 + \sqrt{\frac{5}{3}}s_2 \right)$	$v'_e = \left( -\frac{1}{4} + s_\theta^2 \right) / \sqrt{c_{2\theta}}$
$a'_e = \frac{1}{4}s_\theta \left( -\frac{1}{3}c_2 + \sqrt{\frac{5}{3}}s_2 \right)$	$a'_e = -\frac{1}{4}\sqrt{c_{2\theta}}$
$v'_u = 0$	$v'_u = \left( \frac{1}{4} - \frac{2}{3}s_\theta^2 \right) / \sqrt{c_{2\theta}}$
$a'_u = -\frac{1}{3}s_\theta c_2$	$a'_u = \frac{1}{4}\sqrt{c_{2\theta}}$
$v'_d = \frac{1}{4}s_\theta \left( c_2 + \sqrt{\frac{5}{3}}s_2 \right)$	$v'_d = \left( -\frac{1}{4} + \frac{1}{3}s_\theta^2 \right) / \sqrt{c_{2\theta}}$
$a'_d = a'_e$	$a'_d = a'_e$

**Table 1:** Vector and axial-vector couplings for the  $E_6$ -inspired and the LR models,  $s_\theta = \sin\theta$ ,  $s_2 = \sin\theta_2$ ,  $c_2 = \cos\theta_2$ ,  $c_{2\theta} = \cos 2\theta$  with  $\theta_2 = \theta_6 + \tan^{-1} \sqrt{5/3}$  and  $\theta \equiv \theta_W$ .

## 2. $Z'$ Boson studies

One of the simplest extensions of the SM is to introduce an additional  $U(1)$  gauge symmetry, whose breaking scale is close to the Fermi scale. This extra symmetry is predicted in some grand unified theories and in other models. For example, in  $E_6$  scenarios we have the following additional  $U(1)$  current

$$J_{Z'\mu}^f = J_{\chi\mu}^f \cos\theta_6 + J_{\psi\mu}^f \sin\theta_6 \quad (2.1)$$

with different models parameterised by specific values of the angle  $\theta_6$ . The  $\chi, \psi$  and  $\eta$  models correspond to the values  $\theta_6=0$ ,  $\theta_6 = \pi/2$  and  $\theta_6 = -\tan^{-1} \sqrt{5/3}$  respectively. In the LR models, the new  $Z_{LR}$  boson couples to the current

$$J_{Z'\mu} = \alpha_{LR} J_{3R\mu} - \frac{1}{2\alpha_{LR}} J_{(B-L)\mu} \quad (2.2)$$

with  $\alpha_{LR} = \sqrt{g_R^2/g_L^2 \cot^2\theta_W - 1}$ . The vector and axial-vector couplings of the  $Z'$  boson to the SM fermions, for  $E_6$ -inspired and for LR models, are given in Table 1, assuming:

$$J_{Z'\mu}^f = \bar{f} [\gamma_\mu v'_f + \gamma_\mu \gamma_5 a'_f] f \quad (2.3)$$

and the parametrisation  $\theta_2 = \theta_6 + \tan^{-1} \sqrt{5/3}$ . Finally, a useful reference is represented by the so-called sequential standard model (SSM), which introduces an extra  $Z'$  boson with the same couplings of the SM  $Z^0$  boson.

There exist several constraints on the properties of new neutral vector gauge bosons. Direct searches for a new  $Z'$  boson also set lower limits on the masses [4, 5]. These are summarised in Table 2 for various models. An extra  $Z'$  naturally mixes with the SM  $Z^0$  boson. The present precision electroweak data constrain the mixing angle,  $\theta_M$ , within a few mrad, and the masses as shown in Table 2 [6, 7].

A third class of constraints is derived from atomic parity violation (APV) data. We update here the bounds obtained in [8] and based on the 1999 result of weak charge  $Q_W$  in the Cesium atomic parity experiment [9], which indicated a  $\simeq 2.6\sigma$  discrepancy w.r.t. the SM prediction. A series of theoretical papers have since improved the prediction of

$Q_W$ , by including the effect of the Breit interaction among electrons [10] and by refining the calculation of radiative corrections [11]. A complete re-analysis of the parity non conserving amplitude for the  $6S \rightarrow 7S$  transition in Cesium has been performed [12], which improves on the theoretical uncertainties. In addition the self-energy and vertex QED radiative corrections have been shown to yield a large negative contribution to the parity non conserving amplitude [13], bringing the result on the extraction of  $Q_W$  from the Cesium data to:

	$\chi$	$\psi$	$\eta$	$LR$	SSM
CDF	595	590	620	630	690
LEP	673	481	434	804	1787

**Table 2:** 95% C.L. limit on  $M_{Z'}$  (GeV) from  $\sigma(pp \rightarrow Z')B(Z' \rightarrow ll)$  (CDF data) and from the average of the four LEP experiments, for the mixing angle  $\theta_M = 0$ .

$$Q_W = -72.71 \pm 0.29_{\text{exp}} \pm 0.39_{\text{theor}} \quad (2.4)$$

The corresponding SM prediction, obtained for  $m_t=175.3 \pm 4.4$  GeV and  $M_H=(98^{+51}_{-35})$  GeV, is  $Q_W^{(\text{SM})} = -73.10 \pm 0.03$ [14]. Here we inflate the uncertainty to  $\pm 0.13$  to account for the hadronic-loop and other uncertainties. The

new result given in eqs. (2.4) agrees well with the SM prediction. Models involving extra neutral vector bosons can modify the  $Q_W$  value significantly. Assuming no  $Z^0 - Z'$  mixing, the contribution to the weak charge due to the direct exchange of the  $Z'$  is given by

$$\delta_N Q_W = 16a'_e[(2Z + N)v'_u + (Z + 2N)v'_d] \frac{M_Z^2}{M_{Z'}^2} \quad (2.5)$$

where  $Z = 55$ ,  $N = 78$  for Cs and  $a_f, v_f, a'_f, v'_f$  are the  $Z^0$  and  $Z'$  couplings to fermions (see Table 1). For  $E_6$ -inspired models, bounds on  $M_{Z'}$  are derived as function of the angle  $\theta_6$ , by comparing the predicted value for the weak charge with that in eq. (2.4) (see Figure 1). The lower limits on  $M_{Z'}$  are less stringent than, or comparable to those in Table 2. However, as these bounds are very sensitive to the actual value of  $Q_W$  and its uncertainties, further determinations may improve the situation.

In the case of the LR model, neglecting mixing and  $W'$  contributions, we get  $\delta_N Q_W = -(M_Z^2/M_{Z'}^2)Q_W^{(\text{SM})}$  [8], corresponding to the 95% C.L. bound,  $M_{Z_{LR}} > 665$  GeV.

Finally, for the SSM  $Z'$  boson we get a contribution  $\delta_N Q_W = (M_Z^2/M_{Z'}^2)Q_W^{(\text{SM})}$  [8], leading to the 95% C.L. bound,  $M_{Z'_{SSM}} > 1010$  GeV.

The LHC hadron collider will push the direct sensitivity to new vector gauge bosons beyond the TeV threshold. With an integrated luminosity of  $100 \text{ fb}^{-1}$ , ATLAS and CMS are expected to observe signals from  $Z'$  bosons for masses up to 4-5 TeV depending on the specific model [15].

Extra- $U(1)$  models can be accurately tested at a future linear  $e^+e^-$  collider, operating in the multi-TeV region, such as CLIC. With an expected effective production cross section  $\sigma(e^+e^- \rightarrow Z'_{SSM})$  of  $\simeq 15$  pb, including the effects of ISR and luminosity spectrum, a  $Z'$  resonance will tower over a  $q\bar{q}$  continuum background of  $\simeq 0.13$  pb. While the observation of such signal is granted, the accuracy that can be reached in the study of its properties depends on the quality of the accelerator beam energy spectrum and on the detector response, including accelerator induced backgrounds. One of the main characteristics of

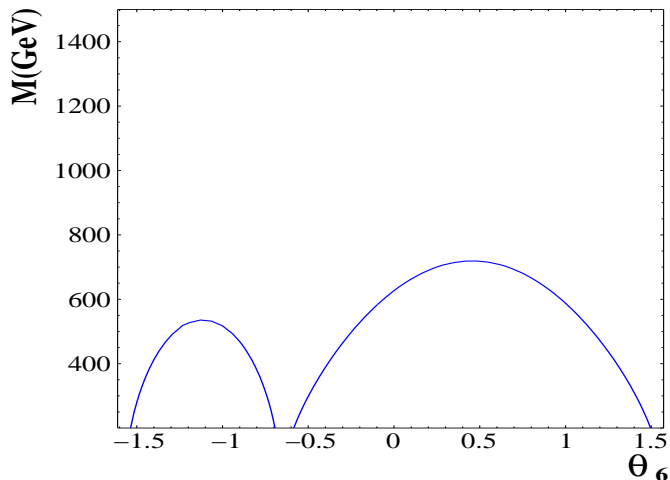


**Figure 1:** 95% C.L. lower bounds on  $M_{Z'}$  at fixed  $\theta_6$  from the Cesium atomic parity experiment result given in eq. (2.4).

the CLIC collider is the large design luminosity,  $L = 10^{35} \text{ cm}^{-2} \text{ s}^{-1}$  at  $\sqrt{s} = 3 \text{ TeV}$  for its baseline parameters, obtained in a regime of strong beamstrahlung effects. The optimisation of the total luminosity and its fraction in the peak has been studied for the case of a resonance scan. The CLIC luminosity spectrum has been obtained with a dedicated beam simulation program [16] for the nominal parameters at  $\sqrt{s} = 3 \text{ TeV}$ . In order to study the systematics from the knowledge of this spectrum, the modified Yokoya-Chen parametrisation [17] has been adopted. In this formulation, the beam energy spectrum is described in terms of  $N_\gamma$ , the number of photons radiated per  $e^\pm$  in the bunch, the beam energy spread in the linac  $\sigma_p$  and the fraction  $\mathcal{F}$  of events outside the 0.5% of the centre-of-mass energy. Two sets of parameters have been considered, obtained by modifying the beam size at the interaction point and therefore the total luminosity and its fraction in the highest energy region of the spectrum: CLIC.01 with  $\mathcal{L}=1.05 \times 10^{35} \text{ cm}^{-2} \text{ s}^{-1}$  and  $N_\gamma=2.2$  and CLIC.02 with  $\mathcal{L}=0.40 \times 10^{35} \text{ cm}^{-2} \text{ s}^{-1}$  and  $N_\gamma=1.2$ . The  $Z'$  mass and width can be determined by performing either an energy scan, like the  $Z^0$  line-shape scan performed at LEP/SLC, and also foreseen for the  $t\bar{t}$  threshold, or an auto-scan, by tuning the collision energy just above the top of the resonance and profiting of the long tail of the luminosity spectrum to probe the resonance peak. For the first method both di-jet and di-lepton final states can be considered, while for the auto-scan only  $\mu^+\mu^-$  final states can provide with the necessary accuracy for the  $Z'$  energy.  $e^+e^- \rightarrow Z'$  events have been generated for  $M_{Z'} = 3 \text{ TeV}$ , including the effects of ISR, luminosity spectrum and  $\gamma\gamma$  backgrounds, assuming SM-like couplings, corresponding to a total width  $\Gamma_{Z'_{SSM}} \simeq 90 \text{ GeV}$ . The resonance widths for extra- $U(1)$  models as well as for other SM extensions with additional vector bosons are shown in Figure 2 as a function of the relevant model parameters.

A data set of  $1 \text{ ab}^{-1}$  has been assumed for the CLIC.01 beam parameters and of  $0.4 \text{ ab}^{-1}$  for CLIC.02, corresponding to one year ( $10^7 \text{ s}$ ) of operation at nominal luminosity. This has been shared in a five point scan (see Figure 3) and  $M_{Z'}$ ,  $\Gamma_{Z'}/\Gamma_{Z^0}$  and  $\sigma_{peak}$  have

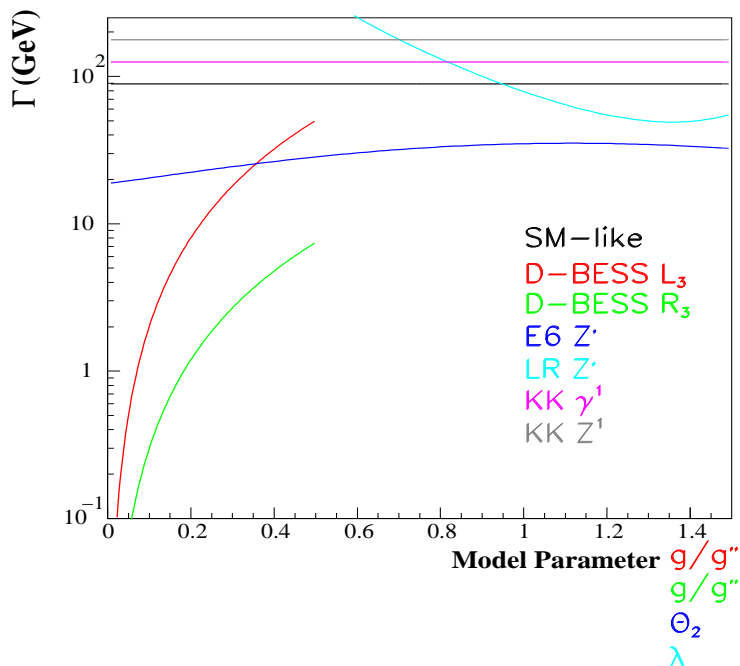


**Figure 2:** Widths of new gauge vector bosons as a function of the relevant parameters:  $\theta_2$  for  $Z'_{E_6}$ ,  $\lambda = g_L/g_R$  for  $Z'_{LR}$  [18],  $g/g''$  for D-BESS. The KK  $Z^{(1)}$  width has a negligible dependence on the mixing angle  $\sin\beta$ . The  $Z'_{E_6}$  and  $Z'_{LR}$  widths are computed by assuming only decays into SM fermions.

Observable	Breit Wigner	CLIC.01	CLIC.02
$M_{Z'}$ (GeV)	$3000 \pm .12$	$\pm .15$	$\pm .21$
$\Gamma_{Z'}/\Gamma_{Z^0}$	$1. \pm .001$	$\pm .003$	$\pm .004$
$\sigma_{peak}^{eff}$ (fb)	$1493 \pm 2.0$	$564 \pm 1.7$	$669 \pm 2.9$

**Table 3:** Results of the fits for the cross section scan of a  $Z'_{SSM}$  obtained by assuming no radiation and ISR with the effects of two different choices of the CLIC luminosity spectrum.

been extracted from a  $\chi^2$  fit to the predicted cross section behaviour for different mass and width values (see Table 3) [19]. The dilution of the analysing power due to the beam energy spread is appreciable, as can be seen by comparing the statistical accuracy from a fit to the pure Born cross section after including ISR and beamstrahlung effects. Still, the relative statistical accuracies are better than  $10^{-4}$  on the mass and  $5 \times 10^{-3}$  on the width. In the case of wide resonances, there is an advantage in employing the broader luminosity spectrum, CLIC.01, which offers larger luminosity. Sources of systematics from the knowledge of the shape of the luminosity spectrum have also been estimated. In order to keep  $\sigma_{syst} \leq \sigma_{stat}$  it is necessary to control  $N_\gamma$  to better than 5% and the fraction  $\mathcal{F}$  of collisions at  $\sqrt{s} < 0.995\sqrt{s_0}$  to about 1% [20].

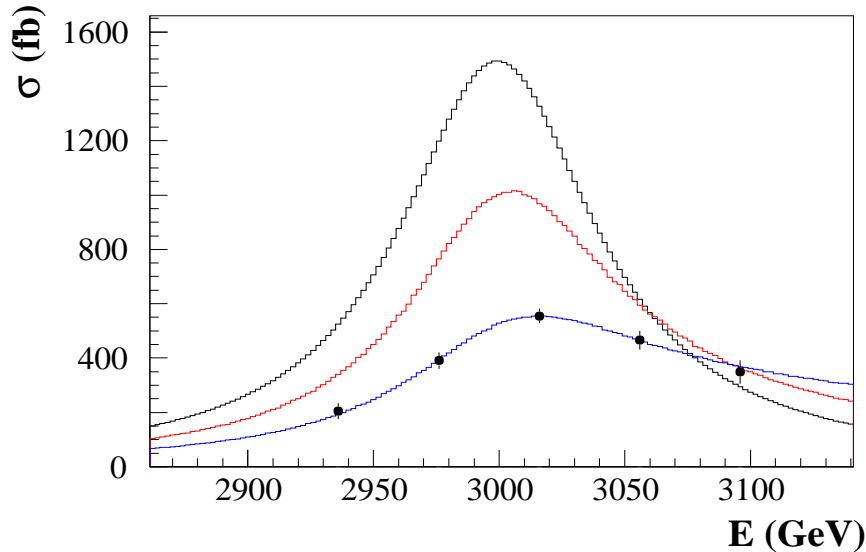


**Figure 3:**  $Z'_{SSM} \rightarrow \ell^+\ell^-$  resonance profile obtained by energy scan. The Born production cross-section, the cross section with ISR included and that accounting for the CLIC luminosity spectrum (CLIC.01) and tagging criteria are shown.

### 3. Study of the D-BESS model

Present precise electroweak data are consistent with the realization of the Higgs mechanism with a light elementary Higgs boson. But as the Higgs boson has so far eluded the direct searches, it remains important to assess the sensitivity of future colliders to strong electroweak symmetry breaking (SSB) scenarios. SSB models are based on low energy effective Lagrangians which provide a phenomenological description of the Goldstone boson dynamics. Possible new vector resonances produced by the strong interaction responsible for the electroweak symmetry breaking can be introduced in this formalism as gauge bosons of a hidden symmetry. A description of a new triplet of vector resonances is obtained by considering an effective Lagrangian based on the symmetry  $SU(2)_L \otimes SU(2)_R \otimes SU(2)_{local}$  [21]. The new vector fields are a gauge triplet of the  $SU(2)_{local}$ . They acquire mass as the  $W^\pm$  and the  $Z^0$  bosons. By enlarging the symmetry group of the model, additional vector and axial-vector resonances can be introduced.

The degenerate BESS model (D-BESS) [2] is a realization of dynamical electroweak symmetry breaking with decoupling. The D-BESS model introduces two new triplets of gauge bosons, which are almost degenerate in mass,  $(L^\pm, L_3), (R^\pm, R_3)$ . The extra parameters are a new gauge coupling constant  $g''$  and a mass parameter  $M$ , related to the scale of the underlying symmetry breaking sector. In the charged sector the  $R^\pm$  fields are not mixed and  $M_{R^\pm} = M$ , while  $M_{L^\pm} \simeq M(1 + x^2)$  for small  $x = g/g''$  with  $g$  the usual  $SU(2)_W$  gauge coupling constant. The  $L_3, R_3$  masses are given by  $M_{L_3} \simeq M(1 + x^2)$ ,  $M_{R_3} \simeq M(1 + x^2 \tan^2 \theta)$  where  $\tan \theta = g'/g$  and  $g'$  is the usual  $U(1)_Y$  gauge coupling constant. These resonances are narrow (see Figure 2) and almost degenerate in mass with  $\Gamma_{L_3}/M \simeq 0.068 x^2$  and  $\Gamma_{R_3}/M \simeq 0.01 x^2$ , while the neutral mass splitting

$g/g''$	$M$ (GeV)	$\Gamma_{L_3}$ (GeV)	$\Gamma_{R_3}$ (GeV)	$S/\sqrt{S+B}$ LHC ( $e + \mu$ )	$\Delta M$ CLIC
0.1	1000	0.7	0.1	17.3	
0.2	1000	2.8	0.4	44.7	
0.1	2000	1.4	0.2	3.7	
0.2	2000	5.6	0.8	8.8	
0.1	3000	2.0	0.3	(3.4)	$23.20 \pm .06$
0.2	3000	8.2	1.2	(6.6)	$83.50 \pm .02$

**Table 4:** Sensitivity to production of the  $L_3$  and  $R_3$  D-BESS resonances at the LHC for  $\mathcal{L}=100(500) \text{ fb}^{-1}$  with  $M=1,2(3) \text{ TeV}$  and accuracy on the mass splitting at CLIC for  $\mathcal{L}=1 \text{ ab}^{-1}$ .

is:  $\Delta M/M = (M_{L_3} - M_{R_3})/M \simeq (1 - \tan^2 \theta) x^2 \simeq 0.70 x^2$ . This model respects the present bounds from electroweak precision data since the  $S, T, U$  (or  $\epsilon_1, \epsilon_2, \epsilon_3$ ) parameters vanish at the leading order in the limit of large  $M$  due to an additional custodial symmetry. Therefore, electroweak data set only loose bounds on the parameter space of the model. We have studied these bounds by considering the latest experimental values of the  $\epsilon$  parameters coming from the high energy data [22]:

$$\epsilon_1 = (5.4 \pm 1.0) \cdot 10^{-3}, \quad \epsilon_2 = (-9.7 \pm 1.2) \cdot 10^{-3}, \quad \epsilon_3 = (5.4 \pm 0.9) \cdot 10^{-3} \quad (3.1)$$

We have included radiative corrections, taken to be the same as in the SM, with the Higgs mass as a cut-off [2]. For  $m_t = 175.3 \text{ GeV}$  and  $m_H = 1000 \text{ GeV}$  one has [23]:  $\epsilon_1^{\text{rad}} = 3.78 \cdot 10^{-3}$ ,  $\epsilon_2^{\text{rad}} = -6.66 \cdot 10^{-3}$ ,  $\epsilon_3^{\text{rad}} = 6.65 \cdot 10^{-3}$ . The 95% C.L. bounds on the parameters of the D-BESS model are shown in Figure 4. Comparable bounds come from the direct search at the TEVATRON [2].

The LHC can discover these new resonances, which are produced through a  $q\bar{q}$  annihilation through their leptonic decay  $q\bar{q}' \rightarrow L^\pm, W^\pm \rightarrow (e\nu_e)\mu\nu_\mu$  and  $q\bar{q} \rightarrow L_3, R_3, Z, \gamma \rightarrow (e^+e^-)\mu^+\mu^-$ . The relevant observables are the di-lepton transverse and invariant masses. The main backgrounds, left to these channels after the lepton isolation cuts, are the Drell-Yan processes with SM gauge bosons exchange in the electron and muon channel. The study has been performed using a parametric detector simulation [24]. Results are given in Table 4 for the combined electron and muon channels for  $\mathcal{L} = 100 \text{ fb}^{-1}$ , except for  $M = 3 \text{ TeV}$  where  $500 \text{ fb}^{-1}$  are assumed.

The discovery limit at LHC, with  $\mathcal{L} = 100 \text{ fb}^{-1}$ , is  $M \sim 2 \text{ TeV}$  for  $g/g'' = 0.1$ . Beyond discovery, the possibility to disentangle the characteristic double peak structure depends strongly on  $g/g''$  and smoothly on the mass.

The LC can also probe this multi-TeV region through the virtual effects in the cross-sections for  $e^+e^- \rightarrow L_3, R_3, Z, \gamma \rightarrow f\bar{f}$ , at centre-of-mass energies below the resonances. Due to the presence of new spin-one resonances the annihilation channel in  $f\bar{f}$  and  $W^+W^-$  has a better sensitivity than the fusion channel. In the case of the D-BESS model, the  $L_3$  and  $R_3$  states are not strongly coupled to  $W$  pairs, making the  $f\bar{f}$  final states the most favourable channel for discovery. Analysis at  $\sqrt{s} = 500 \text{ GeV}$  and  $\sqrt{s} = 800 \text{ GeV}$  is based



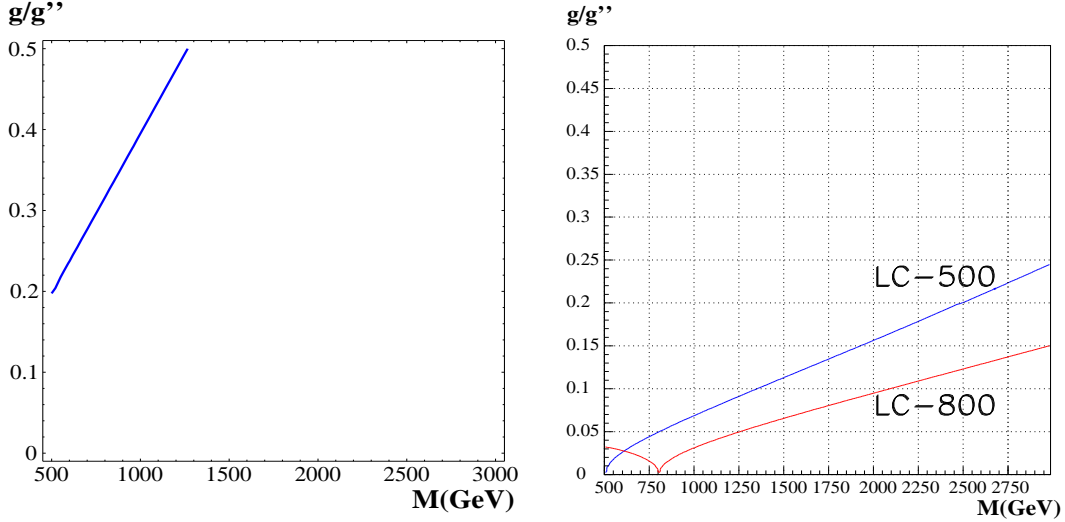


**Figure 4:** 95% C.L. contours in the plane  $(M, g/g'')$  from the present  $\epsilon$  measurements (left-hand side) and from measurements of  $\sigma_{\mu^+\mu^-}$ ,  $\sigma_{b\bar{b}}$ ,  $A_{FB}^{\mu\mu}$ ,  $A_{FB}^{bb}$  at  $e^+e^-$  linear colliders with  $\sqrt{s} = 500(800)$  GeV and  $\mathcal{L} = 1 \text{ ab}^{-1}$  (right-hand side). The allowed regions are below the curves.

on  $\sigma_{\mu^+\mu^-}$ ,  $\sigma_{b\bar{b}}$ ,  $A_{FB}^{\mu\mu}$  and  $A_{FB}^{bb}$ . We assume identification efficiencies of  $\epsilon_\mu = 95\%$  and  $\epsilon_b = 60\%$  and systematic uncertainties of  $\Delta\epsilon_\mu/\epsilon_\mu = 0.5\%$ ,  $\Delta\epsilon_b/\epsilon_b = 1\%$  as.

The sensitivity contours obtained for  $\mathcal{L} = 1 \text{ ab}^{-1}$  are shown in Figure 4. The 3 TeV LC indirect reach is lower or comparable to that of the LHC. However, the QCD background rejection essential for the LHC sensitivity still needs to be validated using full detector simulation and pile-up effects.

Assuming a resonant signal to be seen at the LHC or indirect evidence to be obtained at a lower energy LC, CLIC could measure the width and mass of this state and also probe its almost degenerate structure [25]. This needs to be validated when taking the luminosity spectrum and accelerator induced backgrounds into account. The ability to identify the model distinctive features has been studied using the production cross section and the flavour dependent forward-backward asymmetries, for different values of  $g/g''$ . The resulting distributions are shown in Figure 5 for the case of the narrower CLIC.02 beam parameters. A characteristic feature of the cross section distributions is the presence of a narrow dip, due to the interference of the  $L_3$ ,  $R_3$  resonances with the  $\gamma$  and  $Z^0$  and to cancellations of the  $L_3$ ,  $R_3$  contributions. Similar considerations hold for the asymmetries. In the case shown in Figure 5, the effect is still visible after accounting for the luminosity spectrum. In this analysis, the beam energy spread sets the main limit to smallest mass splitting observable. With realistic assumptions and  $1 \text{ ab}^{-1}$  of data CLIC will be able to resolve the two narrow resonances for values of the coupling ratio  $g/g'' > 0.08$ , corresponding to a mass splitting  $\Delta M = 13 \text{ GeV}$  for  $M = 3 \text{ TeV}$ , and to determine  $\Delta M$  with a statistical accuracy better than 100 MeV (see Table 4).

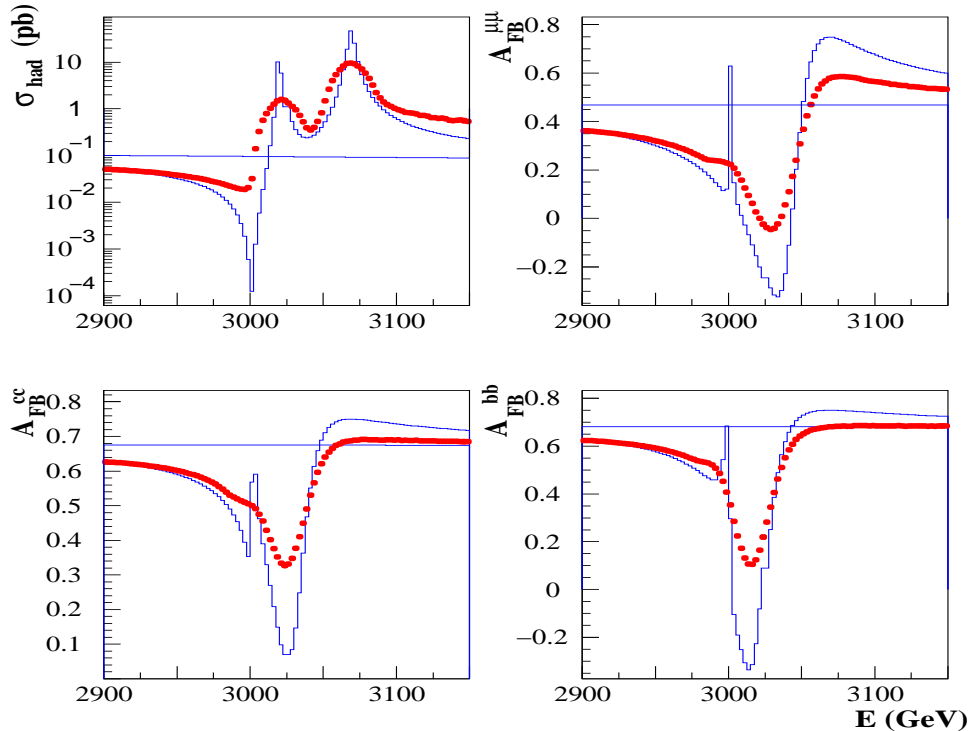


**Figure 5:** Hadronic cross section (upper left) and  $\mu^+\mu^-$  (upper right),  $c\bar{c}$  (lower left) and  $b\bar{b}$  (lower right) forward-backward asymmetries at energies around 3 TeV. The continuous lines represent the predictions for the D-BESS model with  $M = 3$  TeV and  $g/g'' = 0.15$ , the flat lines the SM expectation and the dots the observable D-BESS signal after accounting for the CLIC.02 luminosity spectrum.

#### 4. Kaluza-Klein excitations in theories with Extra-Dimensions

Theories of quantum gravity have considered the existence of extra-dimensions for achieving the unification of gravity at a scale close to that of electroweak symmetry breaking. String theories have recently suggested that the SM could live on a  $3 + \delta$  brane with  $\delta$  compactified large dimensions while gravity lives on the entire ten dimensional bulk. The corresponding models lead to new signatures for future colliders ranging from Kaluza-Klein (KK) excitations of the gravitons [26] to KK excitations of the SM gauge fields with masses in the TeV range [27].

Among the models with extra dimensions we consider here a five-dimensional extension of the SM with fermions on the boundary. This predicts KK excitations of the SM gauge bosons with fermion couplings  $\sqrt{2}$  larger compared to those of the SM [28]. Masses of KK excitations of  $W$ ,  $Z^0$  and  $\gamma$  are given by  $M_n \simeq nM$ , for large value of the fifth dimension compactification scale,  $M$ .

Indirect limits from electroweak measurements already exist and are derived by considering the modifications in the electroweak observables at the  $Z^0$  peak and at low energy [29, 30]. We discuss here the bounds derived from recent determination of the  $\epsilon$  parameters, given on eq. (3.1), and from the APV results discussed in Section 2.

The contribution of the KK excitations of  $W^\pm$ ,  $Z^0$  and  $\gamma$  to the  $\epsilon$  parameters is given by:

$$\epsilon_{1N} = -c_\theta^2 X [1 + s_\beta^2 \frac{s_\theta^2}{c_\theta^2} (1 + c_\beta^2)], \quad \epsilon_{2N} = -c_\theta^2 X, \quad \epsilon_{3N} = -2c_\theta^2 s_\beta^2 X \quad (4.1)$$

where  $X = \pi^2 M_Z^2 / (3M^2)$ , the effective  $\theta$  angle is defined through  $G_F / \sqrt{2} = e^2 / (8s_\theta^2 c_\theta^2 M_Z^2)$  and  $\beta$  parametrises the mixing between the KK excitations and the SM gauge bosons [30]. Contributions from radiative corrections are included assuming SM values. Additional radiative correction terms could originate from the additional charged and neutral Higgs bosons. These are not included here.

The 95% C.L. lower bounds on the scale  $M$  at fixed  $s_\beta$ , coming from the  $\epsilon$  observables, are given by the upper curves in Figures 6. The two curves correspond to  $m_t = 175.3$  GeV and  $m_H = 98$  GeV and  $m_H = 180$  GeV. We have used [23]:  $\epsilon_1^{\text{rad}}(98) = 5.66 \cdot 10^{-3}$ ,  $\epsilon_2^{\text{rad}}(98) = -7.56 \cdot 10^{-3}$ ,  $\epsilon_3^{\text{rad}}(98) = 5.07 \cdot 10^{-3}$  and  $\epsilon_1^{\text{rad}}(180) = 5.39 \cdot 10^{-3}$ ,  $\epsilon_2^{\text{rad}}(180) = -7.41 \cdot 10^{-3}$ ,  $\epsilon_3^{\text{rad}}(180) = 5.49 \cdot 10^{-3}$

Bounds can be also obtained from low energy neutral current experiments. An effective current-current interaction Lagrangian was derived in [30]. From this expression we compute the relevant low energy observables. The atomic weak charge  $Q_W$  is given by

$$Q_W = Q_W^{(\text{SM})} [1 + s_\theta^2 X (s_\beta^2 - 1)^2] - 4 \frac{s_\theta^2 c_\theta^2}{c_{2\theta}} Z \Delta \quad (4.2)$$

where  $Q_W^{(\text{SM})}$  has the SM expression for  $Q_W$ ,  $Z$  is the atomic number and  $\Delta = c_\theta^2 X (1 - 2s_\beta^2 - s_\beta^4 s_\theta^2 / c_\theta^2)$ . By using the determinations for the weak charge of the Cs nucleus, given in eq. (2.4), and its SM prediction of  $-73.10 \pm 0.13$ , as in Section 2, we derive 95% C.L. bounds which results significantly below the corresponding high energy limits and are shown by the lower curves in Figure 6.

Non observation of deviations in lepton pair production at LHC can set limits on the compactification scale  $M$ . For example by considering an effective luminosity of  $5 \text{ fb}^{-1}$  one gets a bound of  $M = 6.7$  TeV [31].

At CLIC, the lowest excitations  $Z^{(1)}$  and  $\gamma^{(1)}$  could be directly produced. Their widths are shown in Figure 2. Since the KK excitations of the photon do not mix with the other gauge vectors, the  $\gamma^{(1)}$  width does not depend on  $\beta$ . The  $Z^{(1)}$  width has only a small correction,  $\frac{\delta\Gamma_{Z^{(1)}}}{\Gamma_{Z^{(1)}}} = 2 \sin^2 \beta \frac{m_Z^2}{M^2}$  which is not visible in the Figure.

Results for the  $\mu^+ \mu^-$  cross sections and forward-backward asymmetries at the Born level and after folding the effects of the CLIC.02 beam spectrum are shown in Figure 7. For comparison, we also present curves corresponding to the case where only the  $Z^{(1)}$  excitation is present.

## 5. Electroweak observables and sensitivity to $Z'$ Boson and KK excitations

The design energy of the CLIC collider generally matches the LHC sensitivity to new gauge vector bosons, allowing to systematically study their properties after their initial observation at the CERN hadron collider.

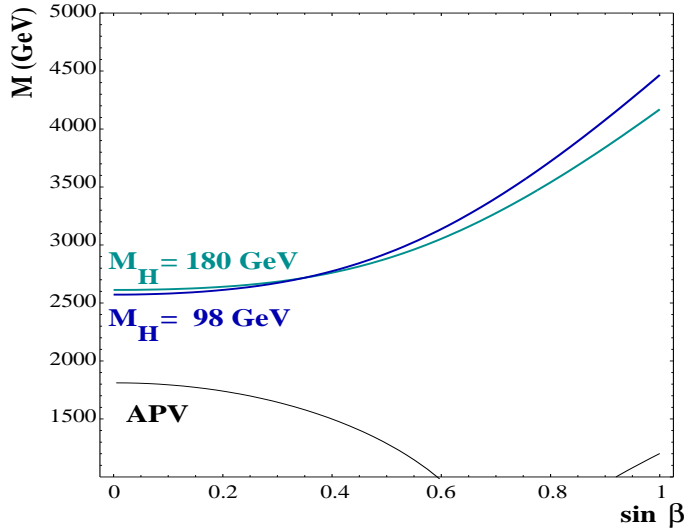


**Figure 6:** 95% C.L. lower bounds on the compactification scale  $M$ , as function of  $\sin \beta$ , from the high energy precision measurements ( $\epsilon$  parameters), for  $m_t = 175.3 \text{ GeV}$  and two different values of  $m_H$  and from the APV data. The regions below the lines are excluded.

Precision electroweak measurements performed in multi-TeV  $e^+e^-$  collisions can push the mass scales sensitivity, for these new phenomena, beyond the 10 TeV frontier. We consider here the  $\mu^+\mu^-$ ,  $b\bar{b}$  and  $t\bar{t}$  production cross sections  $\sigma_{f\bar{f}}$  and forward-backward asymmetries  $A_{FB}^{f\bar{f}}$ . At the CLIC design centre-of-mass energies, the relevant  $e^+e^- \rightarrow f\bar{f}$  cross sections are significantly reduced and the experimental conditions at the interaction region need to be taken into account in validating the accuracies on electro-weak observables. Since the two-fermion cross section is of the order of only 10 fb, it is imperative to operate the collider at high luminosity. This can be achieved only in a regime where beam-beam effects are important and primary  $e^+e^-$  collisions are accompanied by several  $\gamma\gamma \rightarrow$  hadrons interactions. Being mostly confined in the forward regions, this  $\gamma\gamma$  background reduces the polar angle acceptance for quark flavour tagging and dilutes the jet charge separation using jet charge techniques. These experimental conditions require efficient and robust algorithms to ensure sensitivity to flavour-specific  $f\bar{f}$  production. The statistical accuracies for the determination of  $\sigma_{f\bar{f}}$  and  $A_{FB}^{f\bar{f}}$  have been studied using a realistic simulation.  $b\bar{b}$  final states have been identified based on the sampling of the decay charged multiplicity of the highly boosted  $b$  hadrons at CLIC energies [32]. Similarly to LEP analyses, the forward-backward asymmetry for  $b\bar{b}$  has been extracted from a fit to the flow of the jet charge  $Q^{jet}$  defined as  $Q^{jet} = \frac{\sum_i q_i |\vec{p}_i \cdot \vec{T}|^k}{\sum_i |\vec{p}_i \cdot \vec{T}|^k}$ , where  $q_i$  is the particle charge,  $\vec{p}_i$  its momentum,  $\vec{T}$  the jet thrust unit vector,  $k$  a positive number and the sum is extended to all the particles in a given jet. Here the presence of additional particles, from the  $\gamma\gamma$  background, causes a broadening of the  $Q^{jet}$  distribution and thus a dilution of the quark charge separation. The track selection and the value of the power parameter  $k$  need to be optimised as a function of the number of overlaid bunch crossings. Results for the  $e^+e^- \rightarrow t\bar{t}$  channel have been obtained using a dedicated top tagging algorithm [33]. This

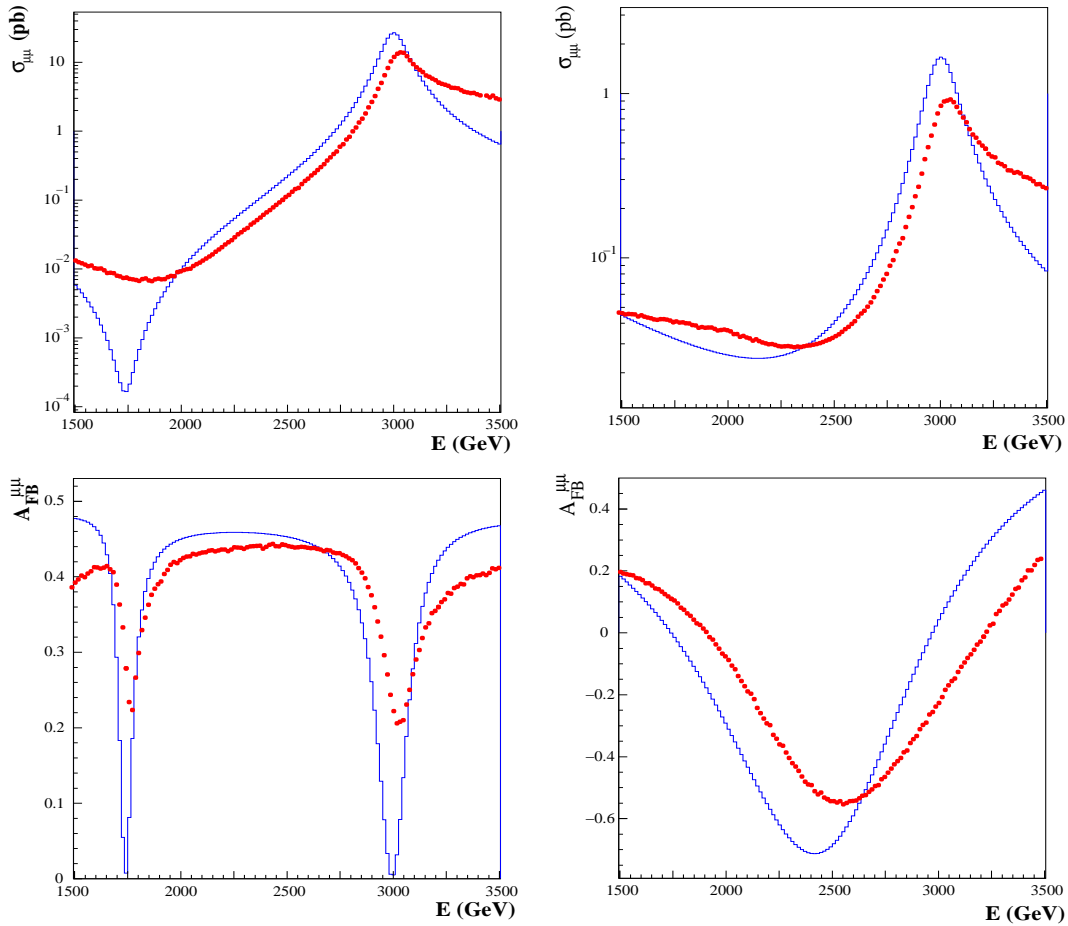


**Figure 7:**  $\mu^+\mu^-$  production cross sections and forward-backward asymmetries in the 5D SM including the lower KK excitations of the  $Z^0$  and  $\gamma$  with  $M_{Z^{(1)}} \sim M_{\gamma^{(1)}} = 3 \text{ TeV}$  (left) and in presence of only the  $Z^{(1)}$  excitation (right). The continuous lines represent the Born-level expectations while the dots include the effect of the CLIC luminosity spectrum.

uses an explicit reconstruction of the  $t \rightarrow bW$  decay and also includes the physics and machine induced backgrounds. For  $t\bar{t}$  forward backward asymmetries the sign of the lepton from the  $W^\pm \rightarrow \ell^\pm \nu$  decay has been used. The results are summarised in terms of the relative statistical accuracies  $\delta\mathcal{O}/\mathcal{O}$  in Table 5.

However, it is important to stress that at the energy scales considered here, electroweak virtual corrections are strongly enhanced by Sudakov double logarithms of the type  $\log^2(s/M_W^2)$ . Until a complete two-loop result will settle the problem, a theoretical error on the cross section of the order of a percent could be considered [34]. We have not included it in the present analysis.

At the LC, the indirect sensitivity to the  $Z'$  mass,  $M_{Z'}$ , can be parametrised in terms of the available integrated luminosity  $\mathcal{L}$ , and centre-of-mass energy,  $\sqrt{s}$ . In fact a scaling law for large  $M_{Z'}$  can be obtained by considering the effect of the  $Z' - \gamma$  interference in the cross section. For  $s \ll M_{Z'}^2$  and assuming that the uncertainties  $\delta\sigma$  are statistically dominated, we get the range of mass values giving a significant difference from the SM

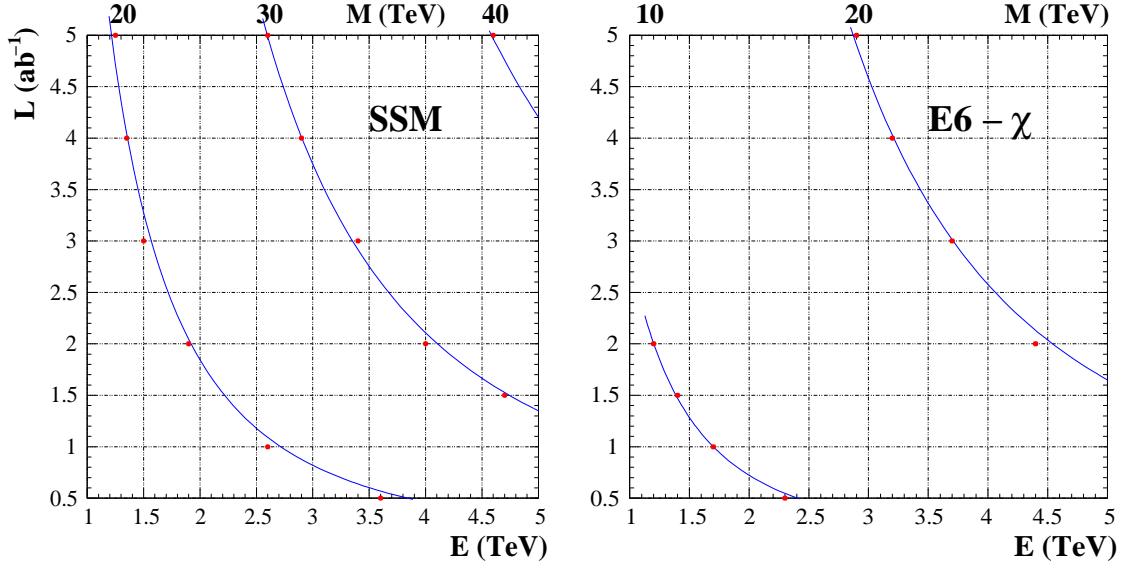


**Figure 8:** The 95% C.L. sensitivity contours in the  $\mathcal{L}$  vs.  $\sqrt{s}$  plane for different values of  $M_{Z'}$  in the SSM model (left) and in the  $E_6 \chi$  model (left). The points represent the results of the analysis, while curves show the behaviour expected from the scaling at eq. (5.2)

prediction:

$$\frac{|\sigma^{SM} - \sigma^{SM+Z'}|}{\delta\sigma} \propto \frac{1}{M_{Z'}^2} \sqrt{s\mathcal{L}} > \sqrt{\Delta\chi^2} \quad (5.1)$$

and the sensitivity to the  $Z'$  mass scales as:

$$M_{Z'} \propto (s\mathcal{L})^{1/4} \quad (5.2)$$

Observable	Relative Stat. Accuracy $\delta\mathcal{O}/\mathcal{O}$ for 1 ab $^{-1}$
$\sigma_{\mu^+\mu^-}$	$\pm 0.010$
$\sigma_{b\bar{b}}$	$\pm 0.012$
$\sigma_{t\bar{t}}$	$\pm 0.014$
$A_{FB}^{\mu\mu}$	$\pm 0.018$
$A_{FB}^{bb}$	$\pm 0.055$
$A_{FB}^{tt}$	$\pm 0.040$

**Table 5:** Relative statistical accuracies on electro-weak observables, obtained for 1 ab $^{-1}$  of CLIC data at  $\sqrt{s} = 3$  TeV, including the effect of  $\gamma\gamma \rightarrow$  hadrons background.

This relationship shows that there is a direct trade-off possible between the centre-of-mass energy,  $\sqrt{s}$ , and the luminosity,  $\mathcal{L}$ , which should be taken into account when optimising the parameters of a high energy  $e^+e^-$  linear collider.

The  $\sigma_{f\bar{f}}$  and  $A_{FB}^{f\bar{f}}$  ( $f = \mu, b, t$ ) values have been computed, for 1 TeV  $< \sqrt{s} < 5$  TeV, both in the SM and including the corrections due to the presence of a  $Z'$  boson with 10 TeV  $< M_{Z'} < 40$  TeV, with couplings defined by the models discussed in Section 2. Predictions have been obtained by implementing these models in the COMPHEP

program [35]. Relative statistical errors on the electroweak observables are obtained by rescaling the values of Table 5 for different energies and luminosities. The sensitivity has

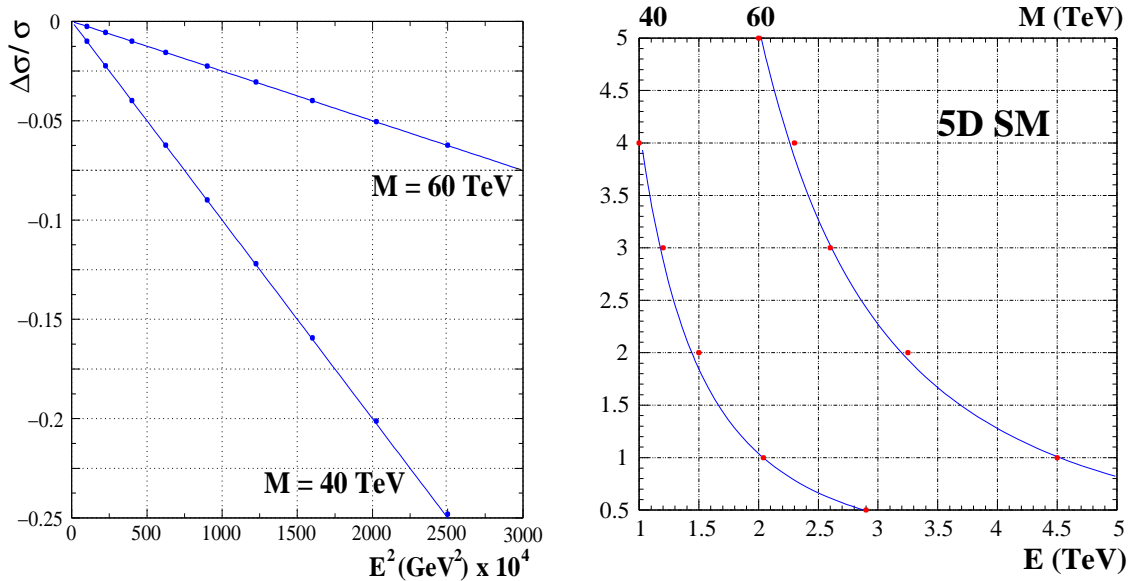


**Figure 9:** Left: Scaling of the relative change for the  $e^+e^- \rightarrow b\bar{b}$  cross section, for the 5D SM, as a function of the square of the centre-of-mass energy, for two values of the compactification scale  $M$ . Right: The 95% C.L. sensitivity contours in the  $\mathcal{L}$  vs.  $\sqrt{s}$  plane for different values of the compactification scale  $M$  in the 5D SM. The points represent the results of the analysis, while curves show the behaviour expected from the scaling in eq. (5.2)

been defined as the largest  $Z'$  mass giving a deviation of the actual values of the observables from their SM predictions corresponding to a SM probability of less than 5%. The SM probability has been defined as the minimum of the global probability computed for all the observables and that for each of them, taken independently.

This sensitivity has been determined, as a function of the  $\sqrt{s}$  energy and integrated luminosity  $\mathcal{L}$  and compared to the scaling in eq. (5.2). Results are summarised in Figure 8. For the  $\eta$  model the sensitivity is lower: for example to reach a sensitivity of  $M_{Z'}=20 \text{ TeV}$ , more than  $10 \text{ ab}^{-1}$  of data at  $\sqrt{s}=5 \text{ TeV}$  would be necessary.

In the case of the 5D SM, we have included only the effect of the exchange of the first KK excitations  $Z^{(1)}$  and  $\gamma^{(1)}$ , neglecting that of the remaining excitations of the towers, which give only small corrections. The scaling law for the limit on  $M$  can be obtained by considering the interference of the two new nearly degenerate gauge bosons with the photon in the cross section and taking the  $s \ll M^2$  limit. The result is the same as eq. (5.2). The analysis closely follows that for the  $Z'$  boson discussed above. In Figure 9 we give the sensitivity contours as a function of  $\sqrt{s}$  for different values of  $M$ . We conclude that the sensitivity achievable on the compactification scale  $M$  for an integrated luminosity of  $1 \text{ ab}^{-1}$  in  $e^+e^-$  collisions at  $\sqrt{s} = 3\text{-}5 \text{ TeV}$  is of the order of 40-60 TeV. Results for a similar analysis, including all electro-weak observables, are discussed in [36].

An important issue concerns the ability to probe the models, once a significant discrepancy from the SM predictions would be observed. Since the model parameters and the mass scale are *a priori* arbitrary, an unambiguous identification of the scenario realised

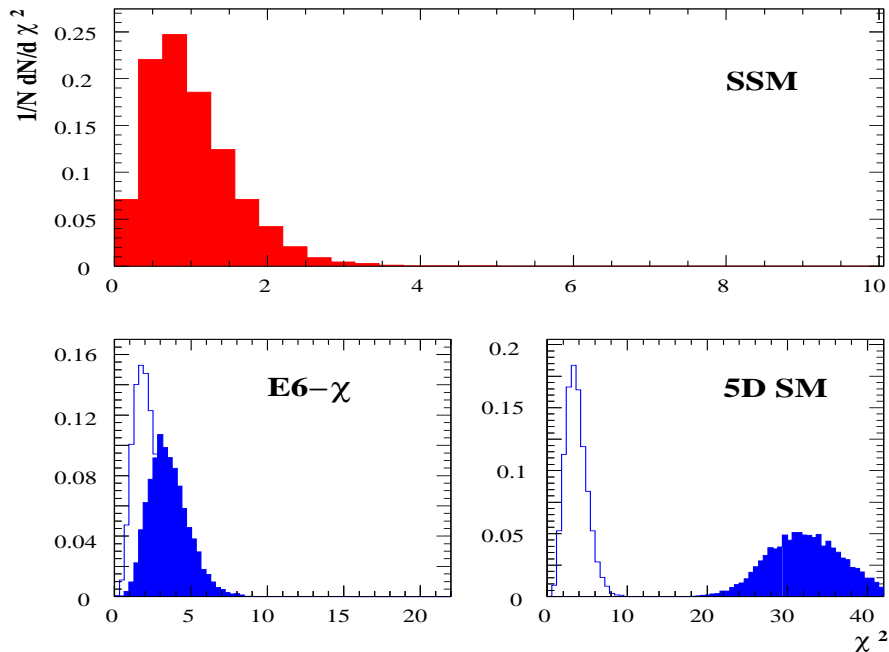


**Figure 10:**  $\chi^2$  distributions obtained for a set of pseudo-experiments where the SSM is realised with a  $M_{Z'}$  mass of 20 TeV (upper plot). The corresponding distributions for the  $E(6) \chi$  and 5D SM for the same mass scale (full histograms) and for  $M=40$  TeV are also shown for comparison in the lower panels. By integrating these distributions, the confidence levels for discriminating between these models, discussed in the text, are obtained.

is difficult. However, some informations can be extracted by testing the compatibility of different models while varying the mass scale. Figure 10 shows an example of such tests. Taking  $M=20$  TeV,  $\mathcal{L} = 1 \text{ ab}^{-1}$  of CLIC data at  $\sqrt{s}=3$  TeV could distinguish the SSM model from the  $E_6 \chi$  model at the 86% C.L. and from the 5D SM at the 99% C.L. For a mass scale of 40 TeV,  $\mathcal{L} = 3 \text{ ab}^{-1}$  of CLIC data at  $\sqrt{s}=5$  TeV, the corresponding confidence levels become 91% and 99% respectively. Further sensitivity to the nature of the gauge bosons could be obtained by studying the polarised forward-backward asymmetry  $A_{FB}^{pol}$  and the left-right asymmetry  $A_{LR}$  colliding polarised beams.

## 6. Conclusions

New neutral vector gauge bosons characterise several extensions of the Standard Model and may represent the main phenomenology beyond 1 TeV. Their existence and properties can be precisely studied at a multi-TeV  $e^+e^-$  collider. Present bounds are derived from precision electro-weak data and typically constrain the masses of these new bosons to be heavier than 1 TeV. At these scales, they may be first observed at the LHC and subsequently studied at CLIC. Accuracies achievable for the determination of their fundamental properties are discussed for different classes of models, using realistic assumptions for the experimental conditions at CLIC. Even beyond the kinematical reach for s-channel pro-



duction, a multi-TeV  $e^+e^-$  collider could probe the existence of new vector resonances up to scales of several tens of TeV by studying the unpolarised electroweak observables. Some information regarding the nature of these new resonances could still be gained and further sensitivity would be provided by the use of polarised beams.

During the completion of this work two papers have confirmed the results on the relevance of the QED self energy and vertex corrections in the calculation of atomic parity violation [37, 38].

It is a pleasure to thank R. Casalbuoni, A. De Roeck, J. Hewett, S. Riemann, T. Rizzo, L. Salmi and D. Schulte for discussion and suggestions on several of the topics presented in this paper.

## References

- [1] *A 3 TeV  $e^+e^-$  Linear Collider Based on CLIC Technology*, G. Guignard (editor), CERN-2000-008.
- [2] R. Casalbuoni, A. Deandrea, S. De Curtis, D. Dominici, F. Feruglio, R. Gatto and M. Grazzini, *Phys. Lett.* **B349** (1995) 533; R. Casalbuoni, A. Deandrea, S. De Curtis, D. Dominici, R. Gatto and M. Grazzini, *Phys. Rev.* **D53** (1996) 5201.
- [3] J. G. Wacker, [arXiv:hep-ph/0208235].
- [4] F. Abe *et al.* [CDF Collaboration], *Phys. Rev. Lett.* **79** (1997) 2192.
- [5] M. Kobel, talk given at the 31st Int. Conference on High Energy Physics, Amsterdam 2002.
- [6] P. Langacker, in *Proc. of the APS/DPF/DPB Summer Study on the Future of Particle Physics (Snowmass 2001)* ed. N. Graf, [arXiv:hep-ph/0110129].
- [7] LEPWWG  $f\bar{f}$  Subgroup, LEP2FF/01-02
- [8] R. Casalbuoni, S. De Curtis, D. Dominici and R. Gatto, *Phys. Lett. B* **460** (1999) 135 [arXiv:hep-ph/9905568].
- [9] S. C. Bennett and C. E. Wieman, *Phys. Rev. Lett.* **82** (1999) 2484 [arXiv:hep-ex/9903022].
- [10] A. Derevianko, *Phys. Rev. Lett.* **85** (2000) 1618; M. G. Kozlov, S. G. Porsev, and I. I. Tupitsyn, *Phys. Rev. Lett.* **86** (2001) 3260; V.A. Dzuba, C. Harabati, W.R. Johnson and M.S. Safronova, *Phys. Rev.* **A63** (2001) 044103.
- [11] A.I. Milstein and O.P. Sushkov, [arXiv:hep-ph/0109257]; W.R. Johnson, I. Bednyakov and G. Soff, *Phys. Rev. Lett.* **87** (2001) 233001.
- [12] V.A. Dzuba, V.V. Flambaum and J.S.M. Ginges, [arXiv:hep-ph/0204134].
- [13] M. Y. Kuchiev and V. V. Flambaum, [arXiv:hep-ph/0206124].
- [14] J. Erler and P. Langacker, in PDG WWW pages (URL:<http://pdg.lbl.gov/>)
- [15] S. Godfrey, in *Proc. of the APS/DPF/DPB Summer Study on the Future of Particle Physics (Snowmass 2001)* ed. N. Graf, [arXiv:hep-ph/0201093].
- [16] D. Schulte, CERN-PS-2001-002-AE *Prepared for 5th International Linear Collider Workshop (LCWS 2000), Fermilab, Batavia, Illinois, 24-28 Oct 2000.*

- [17] K. Yokoya and P. Chen, in Proc. of the *1989 Particle Accelerator Conference*, F. Bennet and L. Taylor (eds.), IEEE 1989 and M. Peskin, LCC Note 0010.
- [18] See for example G. Altarelli *et al.*, Mod. Phys. Lett. **A5** (1990) 495 and Nucl. Phys. **B342** (1990) 15.
- [19] M. Battaglia, S. De Curtis, D. Dominici and S. Riemann, in *Proc. of the APS/DPF/DPB Summer Study on the Future of Particle Physics (Snowmass 2001)* ed. N. Graf, [arXiv:hep-ph/0112270].
- [20] M. Battaglia, S. Jadach and D. Bardin, in *Proc. of the APS/DPF/DPB Summer Study on the Future of Particle Physics (Snowmass 2001)* ed. N. Graf, SNOWMASS-2001-E3015
- [21] R. Casalbuoni, S. De Curtis, D. Dominici and R. Gatto, Phys. Lett. **B155** (1985) 95; *eadem*, Nucl. Phys. **B282** (1987) 235.
- [22] G. Altarelli, F. Caravaglios, G.F. Giudice, P. Gambino and G. Ridolfi, JHEP **0106** (2001) 018.
- [23] G. Altarelli, [arXiv:hep-ph/0011078].
- [24] R. Casalbuoni, S. De Curtis. and M. Redi, Eur. Phys. J. **C18** (2000) 65.
- [25] R. Casalbuoni, A. Deandrea, S. De Curtis, D. Dominici, R. Gatto and J. F. Gunion, JHEP **9908** (1999) 011, [arXiv:hep-ph/9904268].
- [26] G.F. Giudice, R. Rattazzi and J.D. Wells, Nucl. Phys. **B544** (1999) 3; E. A. Mirabelli, M. Perelstein and M. E. Peskin, Phys. Rev. Lett. **82** (1999) 2236; T. Han, J.D. Lykken, R.-J. Zhang, Phys. Rev. **D59** (1999) 105006.
- [27] See, for example, I. Antoniadis, K. Benakli and M. Quiros, Phys. Lett. **B331** (1994) 313, *ibidem* **B460** (1999) 176; T. Rizzo, Phys. Rev. **D64** (2001) 015003.
- [28] A. Pomarol and M. Quiros, Phys. Lett. **B438** (1998) 255 [arXiv:hep-ph/9806263].
- [29] See, for example, T.G. Rizzo and J.D. Wells, Phys. Rev. **D61** (2000) 016007; P. Nath and M. Yamaguchi, Phys. Rev. **D60** (1999) 116006; M. Masip and A. Pomarol, Phys. Rev. **D60** (1999) 096005; A. Strumia, Phys. Lett. **B466** (1999) 107.
- [30] R. Casalbuoni, S. De Curtis, D. Dominici and R. Gatto, Phys. Lett. **B462** (1999) 48 [arXiv:hep-ph/9907355].
- [31] I. Antoniadis, K. Benakli and M. Quiros, Phys. Lett. **B460** (1999) 176 [arXiv:hep-ph/9905311].
- [32] M. Battaglia, in *Physics and Experiments with Future Linear  $e^+e^-$  Colliders*, (A. Para and H.E. Fisk editors), AIP Conference Proceedings, New York, 2001, 813, [arXiv:hep-ex/0011099].
- [33] L. Salmi, in Proc. of the *Workshop on Physics and Experiments with Future Electron-Positron Linear Colliders*, Jeju Island, Korea.
- [34] P. Ciafaloni, [arXiv:hep-ph/0005277] and references therein.
- [35] A. Pukhov *et al.*, INP-MSU-98-41-542, [arXiv:hep-ph/9908288].
- [36] T. G. Rizzo, in *Proc. of the APS/DPF/DPB Summer Study on the Future of Particle Physics (Snowmass 2001)* ed. N. Graf, [arXiv:hep-ph/0108235].
- [37] M. Y. Kuchiev and V. V. Flambaum, [arXiv:hep-ph/0209052].
- [38] A. I. Milstein, O. P. Sushkov and I. S. Terekhov, [arXiv:hep-ph/0208227].